



**HAL**  
open science

## How to build a yeast nucleus

Hua Wong, Jean-Michel Arbona, Christophe Zimmer

► **To cite this version:**

Hua Wong, Jean-Michel Arbona, Christophe Zimmer. How to build a yeast nucleus. *Nucleus*, 2013, 4 (5), pp.361 - 366. 10.4161/nucl.26226 . pasteur-02079519

**HAL Id: pasteur-02079519**

**<https://hal-pasteur.archives-ouvertes.fr/pasteur-02079519>**

Submitted on 26 Mar 2019

**HAL** is a multi-disciplinary open access archive for the deposit and dissemination of scientific research documents, whether they are published or not. The documents may come from teaching and research institutions in France or abroad, or from public or private research centers.

L'archive ouverte pluridisciplinaire **HAL**, est destinée au dépôt et à la diffusion de documents scientifiques de niveau recherche, publiés ou non, émanant des établissements d'enseignement et de recherche français ou étrangers, des laboratoires publics ou privés.



Distributed under a Creative Commons Attribution - NonCommercial - ShareAlike| 4.0  
International License

## How to build a yeast nucleus

Hua Wong, Jean-Michel Arbona, and Christophe Zimmer\*

Institut Pasteur; Unité Imagerie et Modélisation; CNRS URA 2582; Paris, France

**Keywords:** genome architecture, chromosome dynamics, homologous recombination, polymer physics, computational model, nucleolus, chromosome structure, DNA repair, budding yeast, chromosome conformation capture

Submitted: 07/22/13

Accepted: 08/20/13

<http://dx.doi.org/10.4161/nucl.26226>

\*Correspondence to: Christophe Zimmer;  
Email: [czimmer@pasteur.fr](mailto:czimmer@pasteur.fr)

Extra View to: Wong H, Marie-Nelly H, Herbert S, Carrivain P, Blanc H, Koszul R, Fabre E, Zimmer C. A predictive computational model of the dynamic 3D interphase yeast nucleus. *Curr Biol* 2012; 22:1881-90; PMID:22940469; <http://dx.doi.org/10.1016/j.cub.2012.07.069>

**B**iological functions including gene expression and DNA repair are affected by the 3D architecture of the genome, but the underlying mechanisms are still unknown. Notably, it remains unclear to what extent nuclear architecture is driven by generic physical properties of polymers or by specific factors such as proteins binding particular DNA sequences. The budding yeast nucleus has been intensely studied by imaging and biochemical techniques, resulting in a large quantitative data set on locus positions and DNA contact frequencies. We recently described a quantitative model of the interphase yeast nucleus in which chromosomes are represented as passively moving polymer chains. This model ignores the DNA sequence information except for specific constraints at the centromeres, telomeres and the ribosomal DNA (rDNA). Despite its simplicity, the model accounts for a large majority of experimental data, including absolute and relative locus positions and contact frequency patterns at chromosomal and subchromosomal scales. Here, we also illustrate the model's ability to reproduce observed features of chromatin movements. Our results strongly suggest that the dynamic large-scale architecture of the yeast nucleus is dominated by statistical properties of randomly moving polymers with a few sequence-specific constraints, rather than by a large number of DNA-specific factors or epigenetic modifications. In addition, we show that our model accounts for recently measured variations in homologous recombination efficiency, illustrating its potential for quantitatively understanding functional consequences of nuclear architecture.

### Introduction

Several important functions of eukaryotic genomes are affected by the 3D organization of the genome inside the small volume of the nucleus. For example, the chromosomes of higher eukaryotes are organized into distinct nuclear territories, and their relative proximity influences whether loci can undergo illegitimate rejoining events leading up to chromosome translocations, a hallmark of cancer.<sup>1-3</sup> Changes in gene expression are correlated with—and in some cases appear causally linked to—their spatial position relative to coregulated genes or nuclear landmarks such as the nuclear envelope.<sup>4-6</sup> Accordingly, much current research is directed at characterizing genome architecture and at understanding its mechanisms and functional consequences. Fundamental questions remain largely open: where are loci positioned with respect to nuclear landmarks and to each other? How do they move? What determines these positions and movements? In particular, how important are generic properties of polymers as opposed to molecular factors that target specific DNA sequences or epigenetic modulations of chromatin state?<sup>7</sup> How does nuclear organization impact gene expression, DNA replication, repair and recombination?

The humble budding yeast *Saccharomyces cerevisiae* is an important model organism for investigating such questions, owing to its genetic pliability, the relative simplicity of its nuclear architecture and the availability of several quantitative data sets.<sup>7-9</sup> Multiple studies have used this organism to examine the role of nuclear architecture in gene expression and DNA repair.<sup>10-16</sup> Hence, a

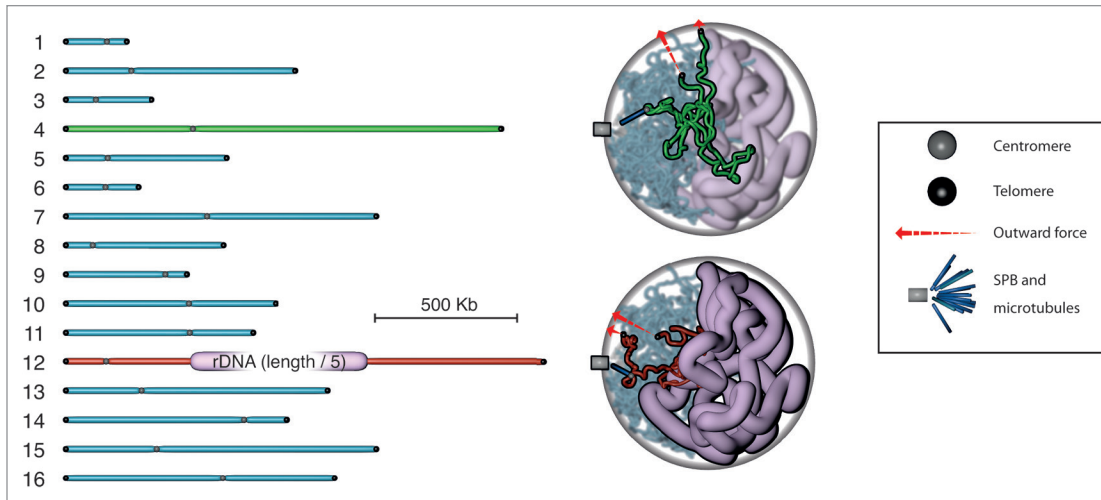


**Figure 1.** Ingredients of a minimal computational model of dynamic chromosome architecture in the budding yeast nucleus.<sup>17</sup> The 16 chromosomes of the haploid yeast genome (shown stretched out on the left), are modeled as random polymer chains undergoing brownian motion and confined to a spherical nucleus (right). Only three DNA sequence-specific constraints are included: centromeres, which are attached to the SPB via short rigid microtubules; telomeres, which are tethered to the nuclear envelope by an outward force; and the rDNA locus, which is modeled as a chain of increased diameter. Chromosomes 4 and 12 are highlighted in the 3D snapshot of the simulation shown on the right.

detailed description and understanding of genome architecture in *S. cerevisiae* is an important objective for the field of nuclear organization at large.

### A Minimal Computational Model of Budding Yeast Nuclear Architecture

We proposed a simple *in silico* model of genome architecture and dynamics for haploid *S. cerevisiae*<sup>17</sup> cells in interphase. The computational recipe for this model can be decomposed as follows:

(1) Treat chromosomes as semi-flexible polymers, modeled as freely jointed chains of non-intersecting rigid segments (Fig. 1). This coarse-grained model of the chromatin fiber neglects all chemical details of the chromosomes and, in particular, ignores the DNA sequence and possible histone modifications. Because the orientation of consecutive segments is random, a given chromosome chain can adopt many different configurations. Modeling chromosomes as freely jointed chains requires assumption of three parameters: (a) the length of each segment, which measures the chain rigidity, (b) DNA compaction, i.e., the number of base pairs corresponding to each segment and (c) the segment diameter. Although these parameters are poorly known *in vivo*,<sup>18,19</sup> we used values derived from the literature, respectively 60

nm, 5 Kb and 20 nm, and applied them to the entire genome (except for the rDNA locus, as detailed in step 5 below).<sup>17</sup> The number of segments in each chromosome is then directly determined by its genomic length and ranges from 46 segments for chromosome 1 (230 Kb) to 306 segments for chromosome 4 (1530 Kb) (Fig. 1).

(2) Enclose the 16 chromosome chains of the haploid yeast genome inside a 2  $\mu$ m diameter sphere representing the nucleus (Fig. 1). Chains are not allowed to intersect each other.

Although step 1 entirely neglected the DNA sequence, we now introduce a minimal set of sequence-specific constraints:

(3) Link the centromeric segment of each chromosome by a single, freely oriented, 380 nm long segment to a single point on the sphere (Fig. 1). This is done because budding yeast centromeres are known to be tethered by a single microtubule to the spindle pole body (SPB), the yeast microtubule organizing center, a protein complex embedded in the nuclear envelope.<sup>7,8</sup>

(4) Apply an outward force to each of the 32 chromosome extremities in order to maintain them near the sphere periphery. This is justified by the fact that telomeres are tethered to the nuclear envelope by two redundant pathways.<sup>20</sup> Since the applied force is purely radial, it does not impose any particular location on the sphere (Fig. 1).

(5) Thicken the rDNA. In *S. cerevisiae*, the genes encoding ribosomal RNA (rDNA) consist of ~100–200 tandem repeats occupying a single locus on the right arm of chromosome 12. The intense transcriptional activity taking place at the rDNA gives rise to the nucleolus, the most conspicuous nuclear structure visible by electron microscopy.<sup>21</sup> The nucleolus represents an obstacle for non-rDNA chromatin and clearly plays a unique role in organizing yeast nuclear architecture.<sup>22,23</sup> Modeling the rDNA in the same manner as other chromosome chains did not allow us to recover observed genome architecture.<sup>17</sup> In order to incorporate the specificity of this locus, we therefore assign a much larger size to rDNA segments (200 nm thick segments instead of 20 nm for all other loci). Qualitatively, this assumption can be justified by the particularly dense accumulation of RNA at this locus, apparent, e.g., from electron micrographs of Miller spreads.<sup>24</sup> The 200 nm value was chosen such that the volume occupied by rDNA segments roughly matched approximately one-third of the nuclear volume, consistent with experimental observations of nucleolar size. Because of this distinct structure for the rDNA locus, chromosome 12 is modeled as a heteropolymer (Fig. 1).

(6) Stir. Starting from an arbitrary initial configuration, let the chromosome

chains move according to pure Brownian dynamics, implying that each segment is displaced in a random direction at each time step, subject only to constraints that maintain chain connectivity and prevent segments from crossing each other (or the spherical boundary). Allow sufficient time for the simulation to run in order to remove the memory of the initial configuration.

Thus, in summary, chromosomes are modeled as confined, randomly moving polymers, with only 3 sequence-specific constraints at the centromeres, telomeres and the rDNA.

### Model Recovers Hallmarks of Yeast Nuclear Architecture

To what extent can such a simple model—that almost completely neglects the genome’s sequence, histone modifications and other functional properties of chromatin—account for observed features of nuclear architecture? To address this, we extensively compared the model’s predictions to experimental measurements, including:

- nuclear territories of 36 distinct loci mapped in 2D by in vivo imaging of thousands of cells.<sup>17,22,25</sup> These loci encompassed 13 out of the 16 chromosomes, included 12 telomeres and 16 loci along the right arm of chromosome 4 (the longest after chromosome 12).
- distributions of distances between 63 pairs of telomeres, also determined by in vivo imaging of thousands of cells.<sup>22</sup>
- contact frequencies across the genome, measured by genome-wide chromosome-conformation capture<sup>23</sup> (Hi-C).

The quantitative nature of these data allowed for statistical analyses of their correlation with model predictions. In summary, we found that:

- The model approximately recovers the nuclear territories of all loci examined and recapitulates the well-known Rabl-like organization of yeast chromosomes.<sup>17,26,27</sup> While some features of this predicted organization—the position of peri-centromeric loci near the SPB, the peripheral localization of telomeres—are rather straightforward consequences of model assumptions (steps 3 and 4 above), the model also makes less obvious

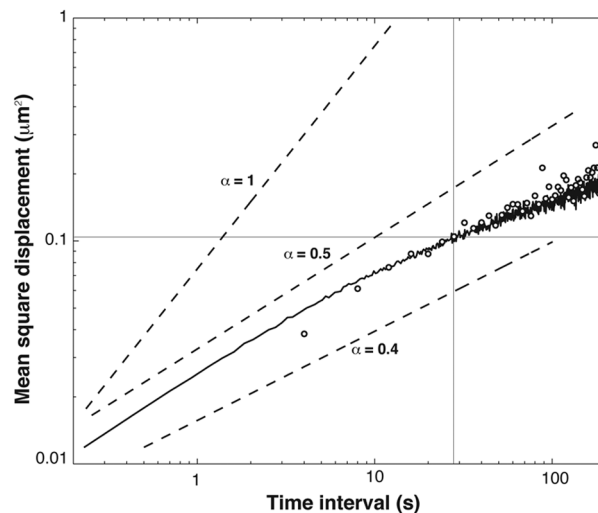


**Figure 2.** Simulated dynamics of the *GAL1* locus agrees with experimental measurements. Mean-square displacements—computed using non-overlapping time intervals—are plotted as function of time interval  $\Delta t$ , for both experimental measurements<sup>11</sup> (white dots) and the simulation<sup>17</sup> (black trace). The time unit for the simulation data was defined such that predicted MSD matched the measurement for  $\Delta t = 28$  s (thin horizontal and vertical lines). The dashed lines correspond to power laws  $\text{MSD}(\Delta t) \propto \Delta t^\alpha$  with  $\alpha = 0.4$ ,  $\alpha = 0.5$  and  $\alpha = 1.0$ . Note that both axes are logarithmic.

predictions. Notably, the predicted territory of rDNA genes adopts a nuclear position opposite the SPB and a crescent-like shape very similar to that actually observed in light or electron microscopy images of the nucleolus.<sup>21,25</sup>

- The predicted nuclear positions of 36 loci—as measured by median angles with respect to a line joining the nuclear and nucleolar centers—correlate well with measured angles (Pearson  $r = 0.87$ ), although a systematic approximately 20 degree shift remains.

- Predicted median distances between 63 pairs of telomeres also correlate well with measurements<sup>22</sup> ( $r = 0.65$ )—despite a systematic difference of  $\sim 150$  nm (and although for a subset of pairs, predictions actually anticorrelate with measurements).

- The predicted proportions of intrachromosomal and interchromosomal contacts (54% and 46%, respectively) agree very well with Hi-C measurements (53% and 47%).<sup>23</sup>

- Predicted mean contact frequencies between pairs of chromosomes correlate very well with Hi-C measurements.<sup>23</sup> This is true regardless of whether interchromosomal or intrachromosomal contacts are taken separately or together (Pearson  $r$  ranging from 0.84 to 0.97). Similar results are obtained when averaging contact

frequencies between all pairs of the 32 chromosome arms.

- Considering the contact frequencies at the finest genomic resolution of our model (5 Kb), the predictions correlate only weakly with the experimental data ( $r = 0.24$ ), but this is plausibly due to the limited signal to noise ratio of the latter. When the genomic bins are increased, however, the correlation improves rapidly ( $r = 0.85$  for bins of 75 Kb).<sup>17</sup>

- The rapidity with which the average intrachromosomal contact frequencies decay as function of the genomic distance  $s$  between loci—an important signature for the physical state of chromosome folding<sup>28,29</sup>—is approximately similar in predictions and measurements, and roughly characterized by a  $s^{-1.5}$  power law followed by an approximate plateau for  $s > 1$  Mb.

- Other predicted patterns of intrachromosomal and interchromosomal contact frequencies also agree with observations, such as the enrichment of contacts between loci at similar distances from their centromere.<sup>23</sup>

- Finally, a recently reported systematic analysis of the territories of 15 loci along chromosome 12 (including 3 rDNA loci) is also in relatively good quantitative agreement with the model’s predictions.<sup>30</sup>

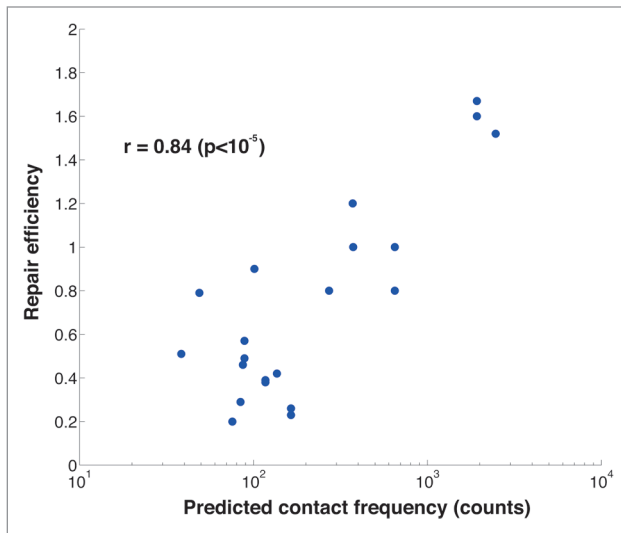


**Figure 3.** Computational prediction of variations in DNA repair efficiency. Experimentally measured efficiencies of homologous recombination<sup>14</sup> are plotted against contact frequencies predicted by our model.<sup>17</sup> Each of the 21 dots corresponds to a distinct pair of homologous loci (some correspond to swapped pairs). The Pearson correlation coefficient between measured efficiencies and predicted contact frequencies is 0.84.

Thus, despite its simplicity, the model accounts to a surprisingly high degree for quantitative measurements of various aspects of genome architecture.

### Predicting Chromatin Dynamics

Chromosomal loci do not remain immobile inside the nucleus but instead undergo motions that have often been described as free diffusion in a confined volume.<sup>16,31-33</sup> Although our model is dynamic, the experimental data discussed above were static, being obtained from Hi-C on formaldehyde-fixed cell populations or from live cell imaging snapshots at a single time point.<sup>22,23,25</sup> However, **Figure 2** illustrates that the model can also be used to successfully predict chromosome dynamics. Specifically, we used the model to compute the mean square displacement (MSD) of the *GALI* locus, as function of time interval  $\Delta t$ . This required a conversion of the simulation time steps into physical time units (seconds). To do this, we defined the physical time of one simulation time step such that the predicted MSD approximately coincided with a previous experimental measurement obtained by single locus tracking<sup>11</sup> for  $\Delta t_i = 28$  s, namely  $\text{MSD}(\Delta t_i) \approx 0.103 \mu\text{m}^2$ . The predicted and measured MSD are shown in **Figure 2**. Although the two curves were

matched at the single time point  $\Delta t_i$ , they are in relatively good agreement over the entire time range shown ( $\Delta t = 4\text{--}200$  s). As apparent from **Figure 2**, both the predicted and observed MSD over this time interval are roughly consistent with a power-law dependence  $\text{MSD}(\Delta t) = C\Delta t^\alpha$ , where  $C$  is a constant and the exponent  $\alpha$  lies between 0.4 and 0.5. Free diffusion is characterized by an exponent  $\alpha = 1$ , while exponents  $\alpha < 1$  indicate subdiffusion. Subdiffusive motions are consistent with expectations from polymer physics. Indeed, because loci are parts of a chain, they are not expected to undergo free diffusion. Instead, the classical Rouse theory of polymer dynamics predicts subdiffusion with  $\alpha = 0.5$  for sufficiently short time intervals  $\Delta t$ .<sup>34-36</sup> The subdiffusive appearance of experimentally measured locus dynamics was previously pointed out,<sup>11</sup> and a recent report provides more extensive evidence for subdiffusive behavior of multiple loci over wider time ranges.<sup>30</sup> Thus, our model also appears able to quantitatively account for observed features of chromosome dynamics.

### Predicting Nuclear Reorganization When Downsizing the Nucleolus

Can the model be used to predict changes in nuclear architecture related

to a functional process? As a first step to address this question, we examined the impact of reducing the volume of the nucleolus, a main determinant of chromosome positioning according to our model. Experimentally, the nucleolar volume can be reduced by treating cells with rapamycin.<sup>22</sup> In our model, this was simulated by reducing the diameter of the rDNA chain segments, while keeping other model parameters unchanged. The resulting model predicted a displacement of telomeres further away from the SPB that agreed with prior observations.<sup>22</sup> This provides a first indication that the model can predict alterations of nuclear architecture resulting from a biological perturbation.

### Predicting Variations in Homologous Recombination Efficiency

Can the model be used to quantitatively understand a functional process that depends on nuclear architecture? One critical nuclear function is the maintenance of genome integrity: genomes are subject to various types of damages, and cells have accordingly evolved mechanisms to repair them. Among the worst damages to the DNA are those that cut both strands of the double helix (double strand breaks, DSB). In yeast, these breaks are repaired mainly by recombination of the broken site with a homologous sequence located elsewhere in the genome. How these matching sequences find each other in nuclear space remains largely unknown.<sup>15,16,37</sup> A recent study investigated the impact of nuclear architecture on the efficiency of DSB repair by homologous recombination.<sup>14</sup> The study relied on yeast strains in which a DSB was induced at a specific site and could be repaired only by recombination with a homologous sequence inserted at another specific locus. The efficiency of repair was then quantified for 21 pairs of loci, involving peri-telomeric, peri-centromeric and some internal loci. In parallel, previous imaging data<sup>22</sup> were used to estimate the degree of overlap between the territories occupied by the two loci in each pair. The measured repair efficiencies correlated well with the estimated territory overlap (Pearson  $r = 0.76$ ,

$p < 10^{-4}$ ): loci sharing similar territories (e.g., two telomeres on short chromosome arms) recombined more frequently than loci whose territories overlapped little (e.g., a telomere on a long arm and a peri-centromeric locus). This argues that homology search is constrained by nuclear architecture and is rate-limiting for homologous recombination.<sup>14</sup>

In **Figure 3**, we plot the measured repair efficiencies<sup>14</sup> against the contact frequencies predicted by our model.<sup>17</sup> The measured efficiencies correlate slightly better with the predicted contact frequencies than with the territory overlaps derived from the images ( $r = 0.84$ ,  $p < 10^{-5}$ ). This suggests that differences in recombination efficiencies can be predicted in absence of imaging or Hi-C data and that our computational model may be relevant for a quantitative understanding of the homology search and DNA repair.

### Related Work

Several computational models of yeast nuclear architecture have been proposed recently.<sup>23,38–40</sup> Some of these used Hi-C data<sup>23,41</sup> to create a static<sup>23</sup> or dynamic 3D model,<sup>38,40</sup> either by turning the measured contact frequencies into spatial constraints and solving an optimization problem<sup>23</sup> or by turning these frequencies into sequence-specific forces, which were then used to bias a dynamic simulation of polymers.<sup>38,40</sup> Two of these studies<sup>38,40</sup> concluded that sequence-specific interactions are required to account for chromosome

positioning or live cell imaging data, in contrast to ours.<sup>17</sup> The reasons for this discrepancy remain to be analyzed and may possibly include the different experimental data considered.<sup>41,42</sup> However, a modeling effort based on geometric constraints and a structure population<sup>39</sup> led to the conclusion that DNA specific interactions are not required to explain most of the experimental data from imaging<sup>22,25</sup> and Hi-C<sup>23</sup>—in accord with our own findings.<sup>17</sup> Differences of our model<sup>17</sup> with the structure population model<sup>39</sup> include the self-consistent prediction of the nucleolar compartment, as well as the ability to predict dynamic features (**Fig. 2**). For a more extensive discussion of these and other computational models of nuclear architecture see, e.g., reference 36.

### Conclusion

We have proposed a minimalistic dynamic model of chromosomes in the yeast nucleus, based on generic polymer physics, which assumes a very small number of sequence-specific constraints and only few parameters (**Fig. 1**). Nonetheless, it can explain a large majority of quantitative data available on yeast nuclear architecture, including locus positions, contact frequencies and motion characteristics (**Fig. 2**). This model can now be used to better understand or even predict multiple aspects of nuclear architecture and their functional consequences. We illustrated this for homologous recombination in DNA repair (**Fig. 3**). It will now be

interesting to further examine the implications of the predicted dynamics on the homology search process.

Further improvements in the model can be contemplated. For example, it remains to be determined whether different parameters or model assumptions could help to reduce remaining systematic discrepancies between predictions and measurements. Higher resolution imaging or Hi-C data should allow to test future extensions of the model to finer genomic scales. Further, it will be important to understand how inducible loci can alter their position in response to transcriptional activation,<sup>11,25,43,44</sup> an observation that the present model—which entirely ignores the expression status of genes—cannot account for. Beyond budding yeast, it will be important to test the generality of our model's assumptions by extending it to other organisms.

### Disclosure of Potential Conflicts of Interest

No potential conflict of interest was disclosed.

### Acknowledgments

We thank Martin Kupiec for providing the repair efficiency data used in **Figure 3**, Ghislain Cabal for the trajectory data used in **Figure 2** and Emmanuelle Fabre for comments. We acknowledge funding by Institut Pasteur, Fondation pour la Recherche Médicale (Equipe FRM) and Agence Nationale de la Recherche (grants ANR-09-PIRI-0024, ANR-11-MONU-020-02, ANR-10-INTB-1401).

### References

- Cremer T, Cremer C. Chromosome territories, nuclear architecture and gene regulation in mammalian cells. *Nat Rev Genet* 2001; 2:292-301; PMID:11283701; <http://dx.doi.org/10.1038/35066075>
- Meaburn KJ, Misteli T, Soutoglou E. Spatial genome organization in the formation of chromosomal translocations. *Semin Cancer Biol* 2007; 17:80-90; PMID:17137790; <http://dx.doi.org/10.1016/j.semcancer.2006.10.008>
- Fudenberg G, Getz G, Meyerson M, Mirny LA. High order chromatin architecture shapes the landscape of chromosomal alterations in cancer. *Nat Biotechnol* 2011; 29:1109-13; PMID:22101486; <http://dx.doi.org/10.1038/nbt.2049>
- Chambeyron S, Da Silva NR, Lawson KA, Bickmore WA. Nuclear re-organisation of the Hoxb complex during mouse embryonic development. *Development* 2005; 132:2215-23; PMID:15829525; <http://dx.doi.org/10.1242/dev.01813>
- Mekhail K, Moazed D. The nuclear envelope in genome organization, expression and stability. *Nat Rev Mol Cell Biol* 2010; 11:317-28; PMID:20414256; <http://dx.doi.org/10.1038/nrm2894>
- Osborne CS, Chakalova L, Brown KE, Carter D, Horton A, Debrand E, Goyenechea B, Mitchell JA, Lopes S, Reik W, et al. Active genes dynamically colocalize to shared sites of ongoing transcription. *Nat Genet* 2004; 36:1065-71; PMID:15361872; <http://dx.doi.org/10.1038/ng1423>
- Zimmer C, Fabre E. Principles of chromosomal organization: lessons from yeast. *J Cell Biol* 2011; 192:723-33; PMID:21383075; <http://dx.doi.org/10.1083/jcb.201010058>
- Taddei A, Schober H, Gasser SM. The budding yeast nucleus. *Cold Spring Harb Perspect Biol* 2010; 2:a000612; PMID:20554704; <http://dx.doi.org/10.1101/cshperspect.a000612>
- Sáez-Vázquez J, Gadal O. Genome organization and function: a view from yeast and Arabidopsis. *Mol Plant* 2010; 3:678-90; PMID:20601371; <http://dx.doi.org/10.1093/mp/ssp034>
- Andrulis ED, Neiman AM, Zappulla DC, Sternglanz R. Perinuclear localization of chromatin facilitates transcriptional silencing. *Nature* 1998; 394:592-5; PMID:9707122; <http://dx.doi.org/10.1038/29100>
- Cabal GG, Genovesio A, Rodriguez-Navarro S, Zimmer C, Gadal O, Lesne A, Buc H, Feuerbacher-Fournier F, Olivo-Marin JC, Hurt EC, et al. SAGA interacting factors confine sub-diffusion of transcribed genes to the nuclear envelope. *Nature* 2006; 441:770-3; PMID:16760982; <http://dx.doi.org/10.1038/nature04752>
- Taddei A, Van Houwe G, Hediger F, Kalck V, Cubizolles F, Schober H, Gasser SM. Nuclear pore association confers optimal expression levels for an inducible yeast gene. *Nature* 2006; 441:774-8; PMID:16760983; <http://dx.doi.org/10.1038/nature04845>
- Therizols P, Fairhead C, Cabal GG, Genovesio A, Olivo-Marin JC, Dujon B, Fabre E. Telomere tethering at the nuclear periphery is essential for efficient DNA double strand break repair in sub-telomeric region. *J Cell Biol* 2006; 172:189-99; PMID:16418532; <http://dx.doi.org/10.1083/jcb.200505159>
- Agmon N, Liefshitz B, Zimmer C, Fabre E, Kupiec M. Effect of nuclear architecture on the efficiency of double-strand break repair. *Nat Cell Biol* 2013; 15:694-9; PMID:23644470; <http://dx.doi.org/10.1038/ncb2745>

15. Dion V, Kalck V, Horigome C, Towbin BD, Gasser SM. Increased mobility of double-strand breaks requires Mec1, Rad9 and the homologous recombination machinery. *Nat Cell Biol* 2012; 14:502-9; PMID:22484486; <http://dx.doi.org/10.1038/ncb2465>
16. Miné-Hattab J, Rothstein R. Increased chromosome mobility facilitates homology search during recombination. *Nat Cell Biol* 2012; 14:510-7; PMID:22484485; <http://dx.doi.org/10.1038/ncb2472>
17. Wong H, Marie-Nelly H, Herbert S, Carrivain P, Blanc H, Koszul R, Fabre E, Zimmer C. A predictive computational model of the dynamic 3D interphase yeast nucleus. *Curr Biol* 2012; 22:1881-90; PMID:22940469; <http://dx.doi.org/10.1016/j.cub.2012.07.069>
18. Joti Y, Hikima T, Nishino Y, Kamada F, Hihara S, Takata H, Ishikawa T, Maeshima K. Chromosomes without a 30-nm chromatin fiber. *Nucleus* 2012; 3:404-10; PMID:22825571; <http://dx.doi.org/10.4161/nucl.21222>
19. Dekker J. Mapping in vivo chromatin interactions in yeast suggests an extended chromatin fiber with regional variation in compaction. *J Biol Chem* 2008; 283:34532-40; PMID:18930918; <http://dx.doi.org/10.1074/jbc.M806479200>
20. Hediger F, Neumann FR, Van Houwe G, Dubrana K, Gasser SM. Live imaging of telomeres: yKu and Sir proteins define redundant telomere-anchoring pathways in yeast. *Curr Biol* 2002; 12:2076-89; PMID:12498682; [http://dx.doi.org/10.1016/S0960-9822\(02\)01338-6](http://dx.doi.org/10.1016/S0960-9822(02)01338-6)
21. Léger-Silvestre I, Trumtel S, Noaillac-Depeyre J, Gas N. Functional compartmentalization of the nucleus in the budding yeast *Saccharomyces cerevisiae*. *Chromosoma* 1999; 108:103-13; PMID:10382072; <http://dx.doi.org/10.1007/s004120050357>
22. Thérizols P, Duong T, Dujon B, Zimmer C, Fabre E. Chromosome arm length and nuclear constraints determine the dynamic relationship of yeast subtelomeres. *Proc Natl Acad Sci U S A* 2010; 107:2025-30; PMID:20080699; <http://dx.doi.org/10.1073/pnas.0914187107>
23. Duan Z, Andronescu M, Schutz K, McIlwain S, Kim YJ, Lee C, Shendure J, Fields S, Blau CA, Noble WS. A three-dimensional model of the yeast genome. *Nature* 2010; 465:363-7; PMID:20436457; <http://dx.doi.org/10.1038/nature08973>
24. French SL, Osheim YN, Schneider DA, Sikes ML, Fernandez CF, Copela LA, Misra VA, Nomura M, Wolin SL, Beyer AL. Visual analysis of the yeast 5S rRNA gene transcriptome: regulation and role of La protein. *Mol Cell Biol* 2008; 28:4576-87; PMID:18474615; <http://dx.doi.org/10.1128/MCB.00127-08>
25. Berger AB, Cabal GG, Fabre E, Duong T, Buc H, Nehrbass U, Olivo-Marin JC, Gadal O, Zimmer C. High-resolution statistical mapping reveals gene territories in live yeast. *Nat Methods* 2008; 5:1031-7; PMID:18978785; <http://dx.doi.org/10.1038/nmeth.1266>
26. Rabl C. über Zellteilung. *Morphologisches Jahrbuch* 1885; 10:214-330
27. Jin QW, Fuchs J, Loidl J. Centromere clustering is a major determinant of yeast interphase nuclear organization. *J Cell Sci* 2000; 113:1903-12; PMID:10806101
28. Lieberman-Aiden E, van Berkum NL, Williams L, Imakaev M, Ragozy T, Telling A, Amit I, Lajoie BR, Sabo PJ, Dorschner MO, et al. Comprehensive mapping of long-range interactions reveals folding principles of the human genome. *Science* 2009; 326:289-93; PMID:19815776; <http://dx.doi.org/10.1126/science.1181369>
29. Rosa A, Becker NB, Everaers R. Looping probabilities in model interphase chromosomes. *Biophys J* 2010; 98:2410-9; PMID:20513384; <http://dx.doi.org/10.1016/j.bpj.2010.01.054>
30. Albert B, Mathon J, Shukla A, Saad H, Normand C, Léger-Silvestre I, Villa D, Kamgoue A, Mozziconacci J, Wong H, et al. Systematic characterization of the conformation and dynamics of budding yeast chromosome XII. *J Cell Biol* 2013; 202:201-10; PMID:23878273; <http://dx.doi.org/10.1083/jcb.201208186>
31. Heun P, Laroche T, Shimada K, Furrer P, Gasser SM. Chromosome dynamics in the yeast interphase nucleus. *Science* 2001; 294:2181-6; PMID:11739961; <http://dx.doi.org/10.1126/science.1065366>
32. Marshall WF, Straight A, Marko JF, Swedlow J, Dernburg A, Belmont A, Murray AW, Agard DA, Sedat JW. Interphase chromosomes undergo constrained diffusional motion in living cells. *Curr Biol* 1997; 7:930-9; PMID:9382846; [http://dx.doi.org/10.1016/S0960-9822\(06\)00412-X](http://dx.doi.org/10.1016/S0960-9822(06)00412-X)
33. Neumann FR, Dion V, Gehlen LR, Tsai-Pflugfelder M, Schmid R, Taddei A, Gasser SM. Targeted INO80 enhances subnuclear chromatin movement and ectopic homologous recombination. *Genes Dev* 2012; 26:369-83; PMID:22345518; <http://dx.doi.org/10.1101/gad.176156.111>
34. Doi M, Edwards AM. *The Theory of Polymer Dynamics*. Oxford (UK): Oxford University Press; 1988.
35. Rosa A, Everaers R. Structure and dynamics of interphase chromosomes. *PLoS Comput Biol* 2008; 4:e1000153; PMID:18725929; <http://dx.doi.org/10.1371/journal.pcbi.1000153>
36. Rosa A, Zimmer C. Computational models of large-scale genome architecture. *International Review of Cell and Molecular Biology* 2013; Forthcoming
37. Barzel A, Kupiec M. Finding a match: how do homologous sequences get together for recombination? *Nat Rev Genet* 2008; 9:27-37; PMID:18040271; <http://dx.doi.org/10.1038/nrg2224>
38. Tokuda N, Terada TP, Sasai M. Dynamical modeling of three-dimensional genome organization in interphase budding yeast. *Biophys J* 2012; 102:296-304; PMID:22339866; <http://dx.doi.org/10.1016/j.bpj.2011.12.005>
39. Tjong H, Gong K, Chen L, Alber F. Physical tethering and volume exclusion determine higher-order genome organization in budding yeast. *Genome Res* 2012; 22:1295-305; PMID:22619363; <http://dx.doi.org/10.1101/gr.129437.111>
40. Gehlen LR, Gruenert G, Jones MB, Rodley CD, Langowski J, O'Sullivan JM. Chromosome positioning and the clustering of functionally related loci in yeast is driven by chromosomal interactions. *Nucleus* 2012; 3:370-83; PMID:22688649; <http://dx.doi.org/10.4161/nucl.20971>
41. Rodley CDM, Bertels F, Jones B, O'Sullivan JM. Global identification of yeast chromosome interactions using Genome conformation capture. *Fungal Genet Biol* 2009; 46:879-86; PMID:19628047; <http://dx.doi.org/10.1016/j.fgb.2009.07.006>
42. Bystrycky K, Laroche T, van Houwe G, Blaszczyk M, Gasser SM. Chromosome looping in yeast: telomere pairing and coordinated movement reflect anchoring efficiency and territorial organization. *J Cell Biol* 2005; 168:375-87; PMID:15684028; <http://dx.doi.org/10.1083/jcb.200409091>
43. Taddei A. Active genes at the nuclear pore complex. *Curr Opin Cell Biol* 2007; 19:305-10; PMID:17467257; <http://dx.doi.org/10.1016/j.ceb.2007.04.012>
44. Egecioglu D, Brickner JH. Gene positioning and expression. *Curr Opin Cell Biol* 2011; 23:338-45; PMID:21292462; <http://dx.doi.org/10.1016/j.ceb.2011.01.001>